

## Accepted Article

**Title:** Effect of the Substituent and Amino Group Position on the Lipase-Catalyzed Resolution of  $\gamma$ -Amino Esters: A Molecular Docking Study Shedding Light on CaLB Enantioselectivity

**Authors:** Marina A. Ortega-Rojas, Edmundo Castillo, Rodrigo Said Razo-Hernández, Nina Pastor, Eusebio Juaristi, and Jaime Escalante

This manuscript has been accepted after peer review and appears as an Accepted Article online prior to editing, proofing, and formal publication of the final Version of Record (VoR). This work is currently citable by using the Digital Object Identifier (DOI) given below. The VoR will be published online in Early View as soon as possible and may be different to this Accepted Article as a result of editing. Readers should obtain the VoR from the journal website shown below when it is published to ensure accuracy of information. The authors are responsible for the content of this Accepted Article.

**To be cited as:** *Eur. J. Org. Chem.* 10.1002/ejoc.202100712

**Link to VoR:** <https://doi.org/10.1002/ejoc.202100712>

# Effect of the Substituent and Amino Group Position on the Lipase-Catalyzed Resolution of $\gamma$ -Amino Esters: A Molecular Docking Study Shedding Light on *Candida antarctica* lipase B Enantioselectivity

Marina A. Ortega-Rojas,<sup>[a]</sup> Edmundo Castillo,<sup>\*[b]</sup> Rodrigo Said Razo-Hernández,<sup>[c]</sup> Nina Pastor,<sup>[c]</sup> Eusebio Juaristi,<sup>[d,e]</sup> and Jaime Escalante<sup>\*[a]</sup>

Dedication. Dedicated to the memory of Professor Ferenc Fülöp.

- [a] Dr. Marina A. Ortega-Rojas; Prof. Dr. Jaime Escalante  
Instituto de Investigación en Ciencias Básicas y Aplicadas, Centro de Investigaciones Químicas  
Universidad Autónoma del Estado de Morelos  
Av. Universidad No. 1001, Col. Chamilpa, C.P. 62210 Cuernavaca, Morelos, México  
E-mail: [marina.ortega@uaem.mx](mailto:marina.ortega@uaem.mx); [jaimesc@uaem.mx](mailto:jaimesc@uaem.mx); <https://www.ciquaem.mx/escalante-garcia-jaime>
- [b] Prof. Dr. Edmundo Castillo  
Departamento de Ingeniería Celular y Biocatálisis  
Instituto de Biotecnología, UNAM  
Apartado Postal 510-3, C.P. 62271 Cuernavaca, Morelos, México  
E-mail: [edmundo@ibt.unam.mx](mailto:edmundo@ibt.unam.mx); <https://www.ibt.unam.mx/perfil/1436/dr-edmundo-castillo-rosales>
- [c] Dr. Rodrigo Said Razo-Hernández; Dr. Nina Pastor  
Instituto de Investigación en Ciencias Básicas y Aplicadas, Centro de Investigación en Dinámica Celular  
Universidad Autónoma del Estado de Morelos  
Av. Universidad No. 1001, Col. Chamilpa, C.P. 62210 Cuernavaca, Morelos, México  
E-mail: [rodrigo.razo@uaem.mx](mailto:rodrigo.razo@uaem.mx); [nina@uaem.mx](mailto:nina@uaem.mx)
- [d] Prof. Dr. Eusebio Juaristi  
Departamento de Química  
Centro de Investigación y de Estudios Avanzados  
Av. Instituto Politécnico Nacional No. 2508, 07360 Ciudad de México, México  
E-mail: [ejarist@cinvestav.mx](mailto:ejarist@cinvestav.mx)
- [e] Prof. Dr. Eusebio Juaristi  
El Colegio Nacional  
Luis González Obregón 23, Centro Histórico, 06020 Ciudad de México, México

Supporting information for this article is available at the end of the document via a link.

**Abstract:** The kinetic resolution of *N*-*tert*-butoxycarbonyl  $\gamma$ -amino methyl esters bearing different stereocenters at alpha ( $\gamma^2$ ), beta ( $\gamma^3$ ), or gamma ( $\gamma^4$ ) positions was carried out by enantioselective hydrolysis with *Candida antarctica* lipase B (CaLB) in 2-methyl-2-butanol solvent. The results show that the process is significantly less enantioselective for the  $\gamma^2$ -amino methyl ester ( $E = 2.5$ ), the  $\gamma^3$ -amino methyl ester ( $E = 7.6$ ), and the  $\gamma^4$ -amino methyl ester ( $E = 8.3$ ) when compared with the kinetic resolution of analogous *N*-protected  $\beta^3$ -amino esters ( $E > 80$ ). Based on these results, molecular docking studies were carried out, through which particular regions in the CaLB catalytic cavity were analyzed. The steric exclusion region composed of Ile189 and Val190 residues, together with the amino bonding region that induces a hydrogen bond with the Asp134 residue, appear to be responsible for the high selectivity in the resolution of carboxylic acid derivatives with beta stereocenters. This interaction is well preserved for  $\beta$ -amino esters as substrates. By contrast,  $\gamma$ -amino esters exhibit greater conformational diversity, so the effectiveness of the interaction is reduced, which apparently is responsible for the loss of enantioselectivity in the resolution process.

## Introduction

The synthesis of pharmacologically active compounds from suitable substrates has a prominent relevance in the food, cosmetics, and pharmaceutical industries. In this regard, a high percentage of pharmacologically active compounds are amines or their amino acid/amino amide derivatives.<sup>[1,2]</sup> The specific connectivity and tridimensional distribution of their different chemical groups define their functional characteristics. Therefore, modern drug synthesis considers, as far as possible, the development of new chiral drugs in the form of a single enantiomer.<sup>[2]</sup> In this sense, the importance of preparing enantiomerically pure amines or their amino acid derivatives is of critical significance.<sup>[1-3]</sup>

At present, the two main strategies for obtaining enantiomerically pure compounds are asymmetric synthesis and the resolution of racemic mixtures.<sup>[4]</sup> In both approaches, biocatalysis and/or biotransformations have been recognized as extremely useful and convenient synthetic tools for preparing chiral amines and their derivatives in high enantiopurity owing to their exquisite

## FULL PAPER

selectivity.<sup>[5]</sup> A particularly successful example is the enzymatic preparation of enantiomerically pure  $\beta$ - and  $\gamma$ -amino acids.<sup>[6]</sup> The extraordinary attention paid to the synthesis of enantiomerically pure  $\beta$ - and  $\gamma$ -amino acids arises from their ubiquity in natural products and their interesting pharmacological and biological activity, exhibited in antibiotics, numerous chiral drugs, and valuable building blocks, for example in oligopeptides.<sup>[3,7,8]</sup> In this regard, the incorporation of  $\beta$ - and  $\gamma$ -amino acids in peptides frequently induces remarkable stability and interesting structural and conformational characteristics.<sup>[8]</sup> On the other hand, the recent interest in the synthesis of enantiomerically pure  $\gamma$ -amino acids is a consequence of their exceptional pharmacological applications, for example as  $\gamma$ -aminobutyric acid derivatives for the treatment of various diseases such as neurodegenerative pathologies, as muscle relaxants,<sup>[9]</sup> or as anticonvulsants bearing anxiolytic and analgesic properties.<sup>[10]</sup>

The enantioselective synthesis of  $\beta$ - and  $\gamma$ -amino acids often involves a multi-step reaction procedure and the use of complex chiral auxiliaries that are not always commercially available.<sup>[3,11]</sup> Recently, several research groups have favored the use of enzymes such as lipases, for resolving racemic  $\beta$ -amino acids.<sup>[6]</sup> By contrast, only in few cases the resolution of  $\gamma$ -amino acids or amino esters has been reported.<sup>[12]</sup> In the last two decades, the use of enzymes in organic synthesis has been increasingly applied to obtain enantiomerically pure compounds, this being due to their high stereoselectivity, catalytic promiscuity, and broad substrate specificity among others.<sup>[13]</sup> Lipases are among the favorite biocatalysts; in particular, CaLB is one of the commercially available enzymes most used in organic synthesis, due to its catalytic promiscuity, high selectivity, remarkable thermostability, and high activity in organic solvents.<sup>[14]</sup> CaLB has been successfully employed in the enantioselective synthesis of pharmaceutical building blocks.<sup>[13d,15]</sup> Due to its remarkable catalytic promiscuity, it has been employed in a wide variety of reactions, such as desymmetrization reactions,<sup>[16]</sup> 1,4-Michael-type additions,<sup>[17]</sup> and particularly in resolution procedures of racemic chiral substrates such as primary amines,<sup>[5b,18]</sup> and secondary alcohols.<sup>[18b,19]</sup> In this regard, it has been established that the catalytic cavity of CaLB is formed by two substrate specific pockets, the acyl pocket and the nucleophile pocket, with the catalytic active site located at the bottom of the pockets.<sup>[14c]</sup>

The mechanisms that govern the enantioselectivity of the nucleophilic resolution reactions of chiral amines and chiral alcohols catalyzed by means of CaLB lipases have been adequately described. Molecular dynamics studies of the observed enantiodiscrimination suggest that the nucleophile pocket is delimited by a Trp104 residue, which is essential for the CaLB stereoselectivity.<sup>[18b,20]</sup> In contrast, in the case of the resolution of chiral carboxylic acids, very few theoretical studies have modeled this phenomenon.<sup>[21]</sup> In general, CaLB has exhibited low selectivity in the resolution of chiral carboxylic acids and their ester or amide derivatives, which was ascribed to a relatively large cavity that results in weaker interactions in the acyl pocket, when compared with those operative in the nucleophile specific pocket.<sup>[20,22]</sup>

Among the most effective cases described for the resolution of carboxylic acid derivatives by means of CaLB are those that involve substrates with  $\alpha$ - and/or  $\beta$ -stereocenters.<sup>[22]</sup> Indeed, CaLB shows high enantioselectivity in the resolution of *N*-protected  $\beta^3$ -amino methyl esters via transesterification ( $E > 98$ ),<sup>[23]</sup> hydrolysis of *N*-protected  $\beta^3$ - and  $\beta^{2,3}$ -amino methyl esters

( $E > 80$ ),<sup>[24,25]</sup> or in the resolution of  $\beta$ -amino esters through acylation reactions by using alkyl methoxyacetates as acylating agents (high ee and moderate conversions).<sup>[6h]</sup>

These reports have shown that the reaction of  $\beta^3$ - and  $\beta^{2,3}$ -amino methyl esters using CaLB is directly influenced by the nature of the substituent at the  $\beta$  position of the carboxylic substrate, and is practically independent of any *N*-protecting group. On the other hand, CaLB catalyzed resolution of carboxylic acid derivatives with  $\gamma$  stereocenters have not yet been fully addressed.<sup>[22]</sup> In this context we performed the enantioselective hydrolysis reaction in 2-methyl-2-butanol (2M2B)<sup>[24]</sup> for the resolution of *N*-tert-butoxycarbonyl (*N*-Boc)  $\gamma$ -amino methyl esters with  $\alpha$  ( $\gamma^2$ ),  $\beta$  ( $\gamma^3$ ) and  $\gamma$  ( $\gamma^4$ ) stereocenters. Indeed, this tertiary alcohol was selected as the reaction medium because lipases do not accept it as substrate. Furthermore, 2M2B increases the simultaneous solubility of the ester substrates and water in the required stoichiometric ratio. Moreover, 2M2B facilitates the recovery of the hydrolyzed products (free acids) that are scarcely soluble in 2M2B. It is worth mentioning that up to now, no molecular docking models related to lipase-catalyzed resolution reactions of  $\alpha$ -,  $\beta$ - and  $\gamma$ -amino acids or amino esters in the acyl pocket have been reported.

In this work, we report the effect of methyl substituents on CaLB-catalyzed resolution of *N*-Boc-protected  $\gamma$ -amino methyl esters bearing  $\alpha$  ( $\gamma^2$ ),  $\beta$  ( $\gamma^3$ ), and  $\gamma$  ( $\gamma^4$ ) stereocenters. By studying the enzymatic enantioselective hydrolysis reaction of these  $\beta$ - and  $\gamma$ -amino methyl esters, we define the structural requirements related to the CaLB-catalyzed resolution of these enantiomeric substrates in the acyl pocket. In addition, with the help of computational molecular docking, theoretical elements are provided for the proper understanding of the structural characteristics that determine the selectivity of CaLB towards  $\gamma^2$ -,  $\gamma^3$ -, and  $\gamma^4$ -methyl esters. The information gathered here constitutes a valuable contribution to the solution of the molecular puzzle associated with the contrasting experimentally examined enzymatic resolution of  $\beta$ - and  $\gamma$ -amino acids or the corresponding amino esters catalyzed by CaLB.

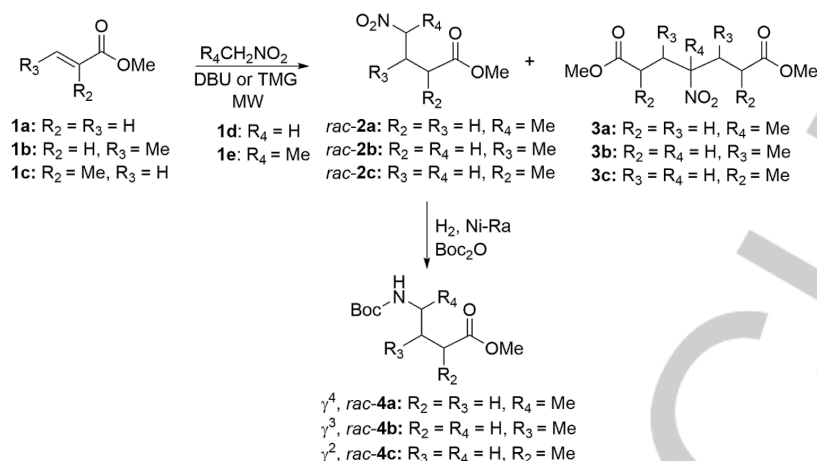
## Results and Discussion

### Chemistry

In order to evaluate the enantioselectivity of CaLB towards the resolution of chiral  $\gamma$ -amino methyl esters, we synthesized different molecules of  $\gamma$ -*N*-Boc-amino methyl esters bearing  $\alpha$  ( $\gamma^2$ ),  $\beta$  ( $\gamma^3$ ) and  $\gamma$  ( $\gamma^4$ ) stereocenters. The synthetic design of the molecules of interest consisted in the incorporation of a methyl group at different positions ( $\alpha$ ,  $\beta$ , or  $\gamma$ ) relative to the carboxylic group. First, the  $\gamma$ -nitro aliphatic methyl esters *rac*-**2a-c** were synthesized by a Michael addition of the corresponding nitronate ions to commercially available acrylates **1a-c**, according to the previously described method (Scheme 1).<sup>[26]</sup>

It is noteworthy that in addition to the anticipated products, double 1,4-addition compounds **3a-c** were also obtained as already reported.<sup>[26]</sup> The direct conversion of  $\gamma$ -nitro aliphatic methyl esters *rac*-**2a-c** to *N*-Boc-amino methyl esters *rac*-**4a-c** was achieved via an efficient one-pot reduction-protection of the nitro group using H<sub>2</sub> and Ni-Ra catalyst in the presence of di-*tert*-butyl dicarbonate (Boc<sub>2</sub>O) as protecting group.

## FULL PAPER



**Scheme 1.** Synthesis of  $\gamma$ -*N*-Boc-amino methyl esters *rac-4a-c* according to the literature.<sup>[26]</sup> MW: Microwave conditions

### Enzymatic resolution

The enantioselectivity of CaLB-catalyzed hydrolysis of  $\gamma$ -*N*-Boc-amino methyl esters *rac-4a-c* (0.2 M) was evaluated in anhydrous 2M2B as solvent; the same methodology used before for the hydrolysis of  $\beta$ -amino esters with  $\beta$  stereocenters.<sup>[24]</sup> The experiments were carried out at 45 °C and at room temperature; reaction progress was followed by <sup>1</sup>H-NMR. Following chromatographic separation of the crude mixture, the enantiomeric excesses (*ee*) for the unreacted amino esters **5a-c** were measured by chiral gas phase chromatography, while the *ee* for the hydrolyzed products **6a-c** were determined by chiral gas phase chromatographic analysis of their ester derivatives **7a-c**. The absolute configurations were assigned by comparison of optical rotation with reported values for the products **6a**,<sup>[8b]</sup> **8a**,<sup>[27]</sup> **6b**, and **6c**<sup>[28]</sup> (Scheme 2).

The hydrolysis reactions at 45°C using  $\gamma^4$ -*rac-4a* as substrate reached conversions of 48 % after 4.5 h, affording the product **6a** with an *ee* of 64 % and values of *E* = 8.3 (entry 2, Table 1). Similar to previous works, these results showed the low selectivity of CaLB for resolving compounds having  $\gamma$  stereocenters.<sup>[22]</sup>

For the racemate  $\gamma^3$ -*rac-4b* bearing the methyl group on the beta position, conversions of 31 % were achieved after 6 h at 45 °C; the hydrolyzed product (*R*)-**6b** was obtained with an *ee* of 70 % and a low *E* value of 7.6 (entry 5, Table 1). Unexpectedly, although CaLB has shown excellent selectivity for derivatives of  $\beta$ -amino esters with  $\beta$ -stereocenters (*E* > 80),<sup>[23-25]</sup> in these reactions, CaLB showed low selectivity for substrate *rac-4b*. Interestingly, while the previously reported resolutions of  $\beta$ -amino esters carry the amino group at the beta position the *rac-4b* substrate of this work carries the amino group at the gamma position.

Finally, in the case of racemate *rac-4c*, where the  $\gamma^2$ -substituent methyl in the  $\alpha$  position was evaluated, the expected reaction proceeded more slowly according to the literature data. The hydrolysis reactions at 45 °C achieved only 31 % conversion after 24 h of reaction; hydrolyzed product (*R*)-**6c** was obtained with an *ee* of 35.6 % and an *E* of 2.5 (entry 8, Table 1).

For the three racemic  $\gamma$ -amino methyl esters *rac-4a-c* that were evaluated CaLB showed poor enantiodiscrimination (*E* value < 10). In order to enhance CaLB enantioselectivity, the hydrolysis reactions of *rac-4a-c* were carried out at room temperature. Unfortunately, the enantioselectivity of these reactions was not improved (entry 3, 6 and 9; Table 1).

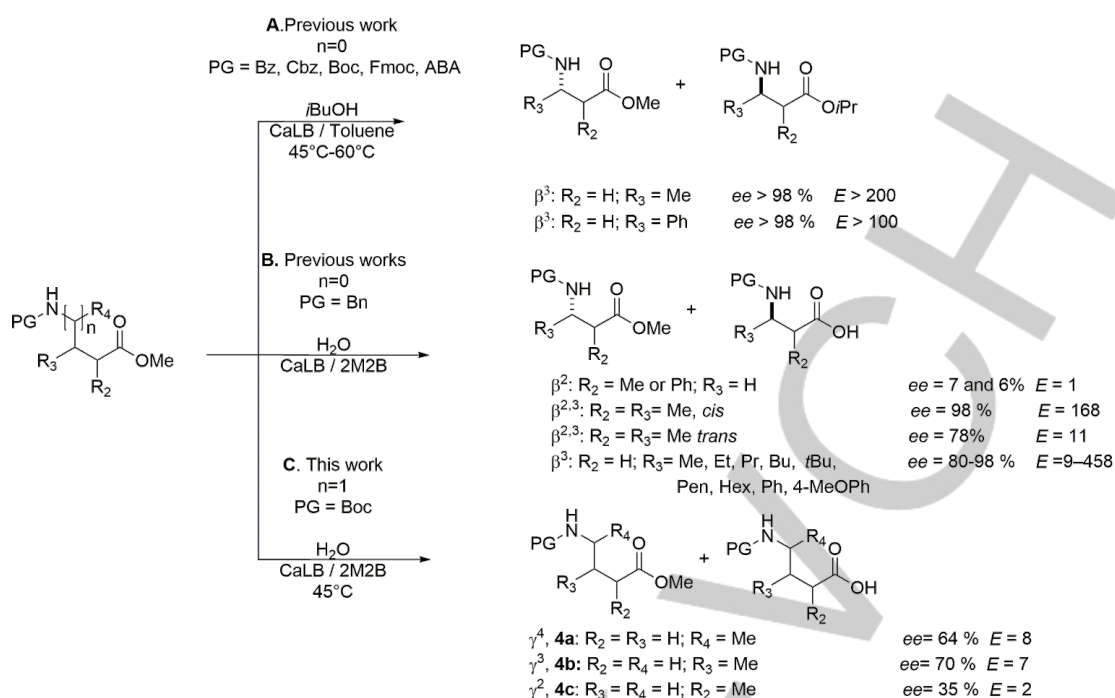
It is worth mentioning that although the values of *ee* and *E* observed for the hydrolyzed product (*R*)-**6a** bearing the stereocenter in  $\gamma$ -position are low, CaLB shows enantioselectivity for the stereoisomer that orients the alkyl substituent out of plane (Scheme 2). In general, these results are in agreement with the low enantioselectivity shown by CaLB in the resolution of carboxylic acid derivatives with  $\gamma$ -stereocenters.<sup>[22]</sup>

Similar enantiodiscrimination was observed for racemic substrates *rac-4b* when the alkyl substituent is located at the  $\beta$  position (Scheme 2). Although the enantioselectivity is in agreement with observation in the resolution of *N*-protected and *N*-benzylated  $\beta^3$ -amino esters,<sup>[23-25]</sup> the lost in enantioselectivity suggests that, in addition to the orientation (configuration) of the alkyl group, the position of the amino group plays an essential role in CaLB enantiodiscrimination.

Finally, for racemic substrate *rac-4c* the hydrolyzed product (*R*)-**6c**, presenting the methyl substituent at the  $\alpha$  position, the enantioselectivity is better with respect to their *N*-benzylated  $\beta^2$ -amino ester analogs,<sup>[24]</sup> and shows an enantioselectivity for the enantiomer with the methyl substituent inside the plane.



## FULL PAPER



**Scheme 3.** Enzymatic resolution of *N*-protected  $\beta^3$ -amino methyl esters (**A**, previous work<sup>[23]</sup>), *N*-benzylated  $\beta^3$ -,  $\beta^{3,2}$ - and  $\beta^2$ -amino methyl esters (**B**, previous works<sup>[24,25]</sup>), and *N*-Boc protected  $\gamma^4$ -,  $\gamma^3$ -,  $\gamma^2$ -amino methyl esters (**C**, this work).

### Molecular modeling

Based on the experimental results of the kinetic resolution of *N*-protected  $\gamma$ -amino methyl esters via enantioselective hydrolysis by means of CaLB (**C**, Scheme 3) and the reports described in the literature for enantioselective transesterification of analogous *N*-protected  $\beta$ -amino methyl esters (**A**, Scheme 3),<sup>[23]</sup> and enantioselective hydrolysis of *N*-benzylated  $\beta$ -amino methyl esters (**B**, Scheme 3),<sup>[24,25]</sup> we carried out a computational molecular docking study examining the structural, complementary requirements in the acyl pocket of the enzyme. This study revealed the non-covalent enzyme-substrate interactions involved in the recognition and formation of the *N*-protected  $\gamma$ -amino ester-CaLB complex before the nucleophilic attack takes place.

The catalytic cavity of CaLB can be visualized as formed by two pockets, the acyl pocket surrounded by Gln157, Asp134, and Thr138, and the nucleophilic pocket delimited by Trp104. The two pockets are separated by several hydrophobic residues with the catalytic triad (Asp187/His224/Ser105) at the bottom of the cavity (Figure 1). For a nucleophilic substitution reaction on the carboxylic group, CaLB acts as chiral catalyst, following an acylation-deacylation dynamic mechanism. In the resolution of the  $\beta$ -amino acid ester as first substrate, Ser105 is activated by the Asp/His residues, thus promoting the nucleophilic attack to the carbonyl carbon of the substrate. The resulting oxyanion is stabilized in the oxyanionic cavity (Gln106, Thr40), while His224 donates the proton to the leaving group of the tetrahedral intermediate. The enzyme generates diastereomeric tetrahedral intermediates of different energies for each of the enantiomeric substrates, which results in the resolution of the racemic mixture (**D** in Figure 1). Electron movement from the negatively charged oxygen to the tetrahedral carbon, induces the release of the leaving group to form the acyl-enzyme intermediate. In the final

step, hydrolysis proceeds via a second tetrahedral intermediate with water as second substrate (nucleophile) to give the hydrolyzed product (Figure 1).<sup>[22]</sup>

The crystal structure of CaLB (PDB: 1LBS) with a phosphonate inhibitor in the catalytic cavity evidenced the mechanism for catalysis via transfer of the histidine proton to the leaving group.<sup>[20]</sup> It is worth mentioning that in the report describing the 1LBS X-ray structure, the authors refer to a mixture of conformations, one with the acyl chain of the substrate in the nucleophilic core of the pocket and the other with the acyl chain of the substrate in the acyl pocket. However, the observed electron density showed that the enzyme was inhibited mainly by the enantiomer whose acyl segment is oriented towards the nucleophilic pocket (PDB: 1LBS). Therefore, it does not form a hydrogen bond with His224, which is essential for a catalytically productive conformation (**F** in Figure 2).

### Validation of the docking protocol

All ligands, including the co-crystallized ligand, were submitted to conformational and structural optimization before docking (for details check the supplementary materials).

The co-crystallized ligand in the CaLB (PDB:1LBS) cavity was well reproduced by its calculated conformation with a value of RMSD = 1.1 Å (**G** in Figure 2). This conformation is a non-productive conformation, as the ethoxy group of the ligand is in the acyl pocket, therefore it does not form a hydrogen bond with the histidine, that is necessary for catalysis. For the study of the active conformation of different ligands, an extra validation methodology was required. In particular, an alternative catalytic conformation for the ligand was calculated, in which the ethoxy group is oriented towards the nucleophile pocket, forming a weak hydrogen bond with the His224 residue (**H** in Figure 2).

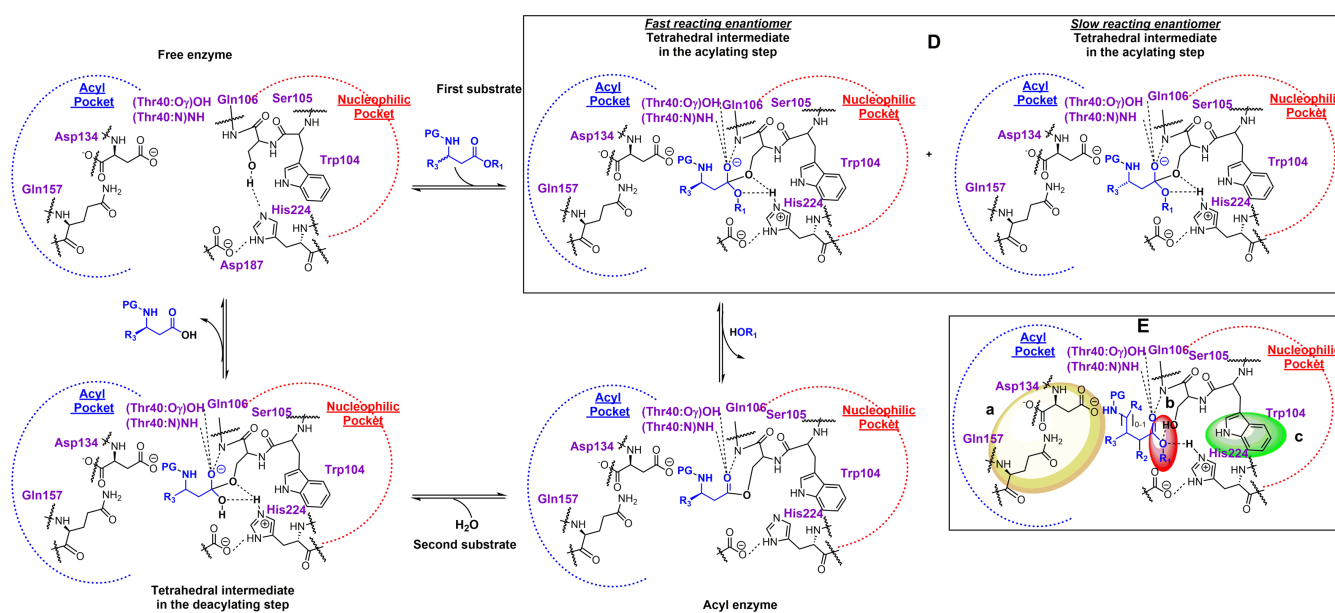


**Figure 1.** Schematic representation of the mechanism of an enzymatic kinetic resolution by CaLB. **D**, Diastereomeric tetrahedral intermediates for each of the enantiomeric substrates, resulting in the required enantiodiscrimination for resolution of the racemic mixture. **E**, Criteria for evaluating the calculated conformations in molecular docking: (a) acyl chain of the ligand surrounded by Asp134/Gln157, (b) hydrogen bond interaction between Ser105 and His224 and the methoxy group at the ligand, (c) the methoxy group of the ligand in the nucleophile pocket delimited by the Trp104 residue.

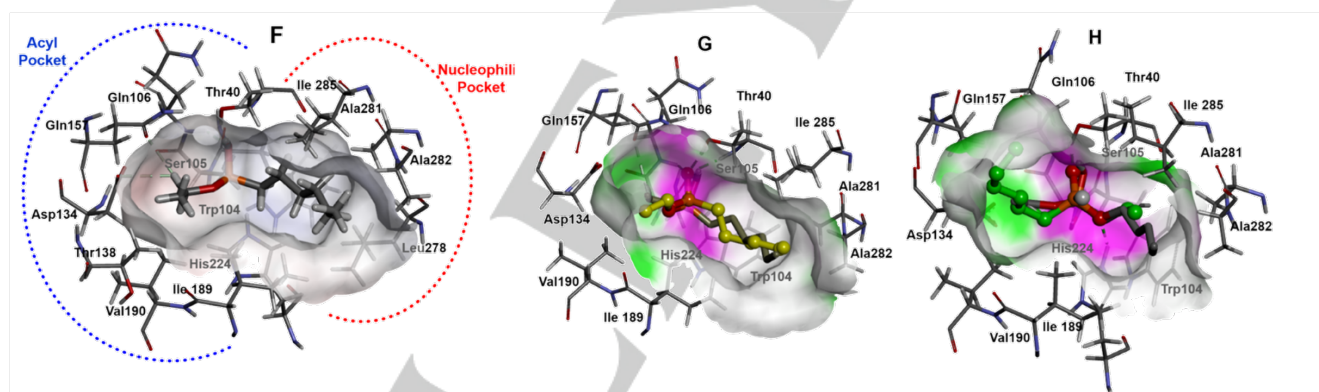


**Figure 2.** **F**, CaLB catalytic cavity (PDB: 1LBS), experimental inhibitor in thick sticks (colored gray), amino acids of the acyl and nucleophilic pockets are displayed. **G**, Comparison of the ligand calculated conformation (sticks and spheres colored yellow) with its crystal conformation (sticks colored gray) (RMSD = 1.1 Å). **H**, Comparison of the ligand calculated conformation (ball and sticks colored green) for a catalytically productive conformation with a hydrogen bond to His224 with its crystal conformation (sticks colored gray). All the residues are represented as thin sticks.

The ligand-protein interaction analysis was based on specific residues, according to the following criteria: a) the ligand's acyl segment should be surrounded by Asp134 and Gln157 (acyl cavity), b) a hydrogen bond interaction between Ser105 and His224 with the methoxy of the ligand, and c) the methoxy group of the ligand in the nucleophile pocket is best delimited by Trp104 (E in Figure 1). Both enantiomers of the substrates were analyzed, according to the following series:  $\beta^3$ - $\gamma$   $\gamma^3$ -amino esters with  $\beta$  stereocenters (Series 1A-C),  $\beta^2$ - and  $\gamma^2$ -amino esters with  $\alpha$  stereocenters (Series 2A and 2B),  $\beta^{2,3}$ -amino esters with  $\beta$   $\alpha$

$\alpha$  stereocenters (Series 3), and the  $\gamma^4$ -amino ester with  $\gamma$  stereocenters (Figure 3). Figure 3 shows the fast-reacting enantiomers.

Docking results were divided in two sections. In the first section, the effect of the size and position of the substituent was analyzed, and in the second section, the position of the amino group was studied. Best ligand-protein interaction energies were obtained for the fast-reacting enantiomers; the energy values can be consulted in the supplementary section.

## FULL PAPER

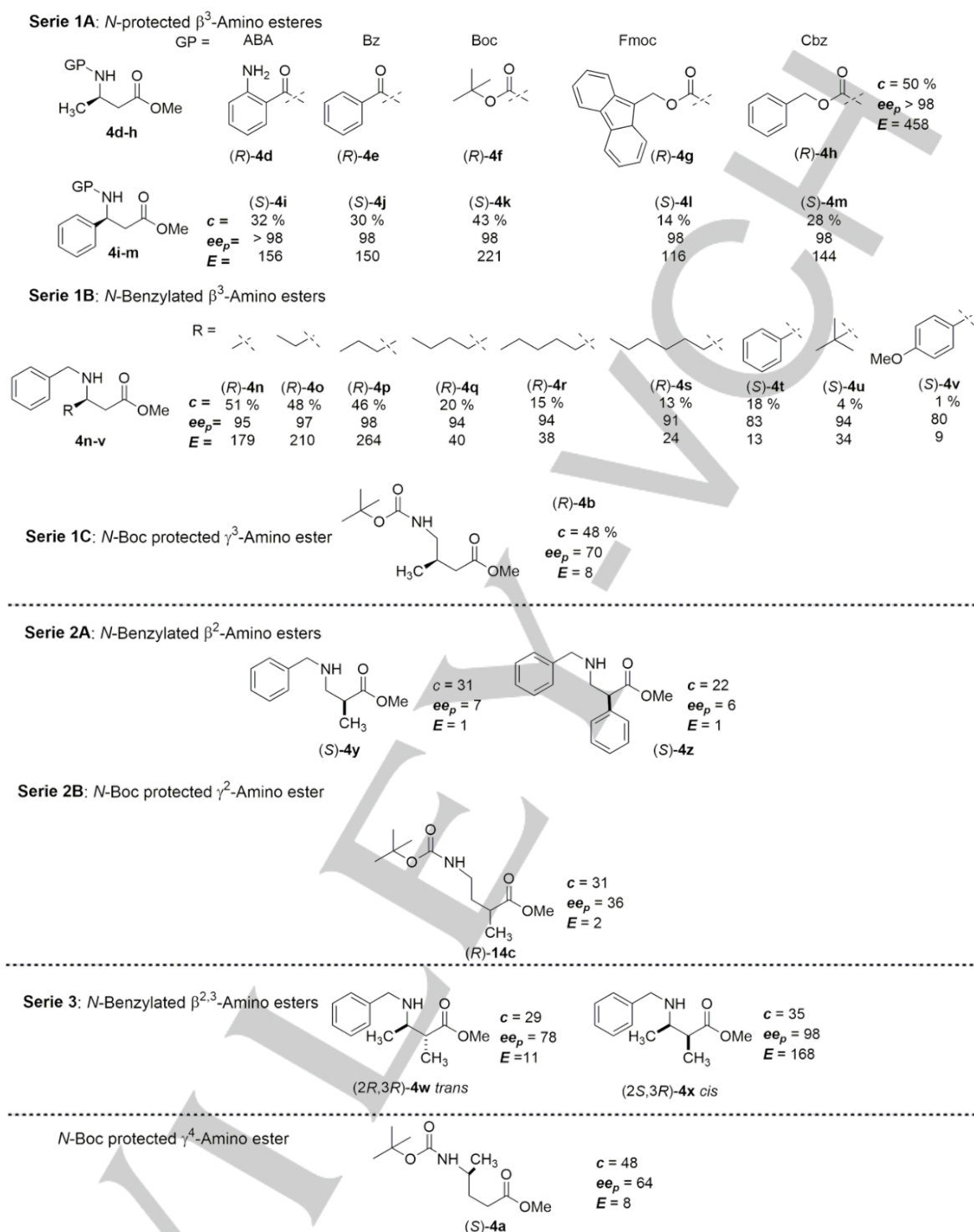


**Figure 3.** Fast reacting enantiomers for: (Series 1A-C)  $\beta^3$ - and  $\gamma^3$ -amino esters with  $\beta$  stereocenters, (Series 2A-B)  $\beta^2$ - and  $\gamma^2$ -amino esters with  $\alpha$  stereocenter, (Series 3)  $\beta^{2,3}$ -amino esters with  $\beta$  and  $\alpha$  stereocenters; and (N-Boc protected  $\gamma^4$ -Amino ester)  $\gamma^4$ -amino ester with  $\gamma$  stereocenter

## FULL PAPER

**Effect of size and position of the substituent**

Molecular docking of the Series 1A-C shows the ability of the ligands to fit into the cavity (shape complementarity) as a determining factor in the reaction rate. Substituents such as phenyl exhibit lower experimental reaction rates and substantial steric congestion in the molecular docking relative to methyl substituents. In addition, the three-dimensional structure of the catalytic cavity can restrict the orientation of the substituents at the stereocenter of the substrate through a steric exclusion effect, as can be seen for the slow reacting enantiomer of *rac*-**4i**. Interactions with Val190, Ile189, and Ser105 show that the fast-reacting enantiomer (*S*)-**4i** orients the phenyl substituent outside the cavity, minimizing steric repulsions. In contrast, the slow reacting (*R*)-**4i** enantiomer suffers steric repulsive interactions with these residues (I in Figure 4). In general, the less active molecules in Series 1A-1C (Figure 3) present steric hindrance with these residues, and show greater conformational distortion (see Supplementary Information).

The calculated conformations for substrates with  $\alpha$  stereocenters in Series 2A-B do not exhibit steric repulsions with the residues of

Ile189 and Val190, but maintain the steric repulsion with catalytic Ser105 (J in Figure 4). Such repulsive interaction can be minimized by optimization of molecular coupling (see Supplementary Information). At the experimental level, substrates with substituents at the  $\alpha$  position show low conversions, long reaction times and low enantiodiscrimination ( $E = 1-2$ ).

The steric repulsion generated by Val190 and Ile189 and the substituent at  $\beta$  position is also observed with *cis*- $\beta^{2,3}$ -amino methyl esters *N*-benzylated (*cis*-**4x**) with  $\alpha$  and  $\beta$  stereocenters (K in Figure 4). The corresponding *trans*-isomers (*trans*-**4w**) showed greater conformational diversity orienting the acyl chain outside of the cavity, minimizing steric repulsions with Val190 and Ile189. At the experimental level, *trans* isomers showed loss of selectivity ( $E = 11$ ) compared to their *cis* counterparts (*cis*-**4x**) ( $E > 100$ ). Finally, the analysis for  $\gamma^4$ -amino esters with  $\gamma$  stereocenters (Series 4, Figure 3) shows that the substituent at position  $\gamma$  does not generate significant steric repulsion with Val190 and/or Ile189 (L in Figure 4).

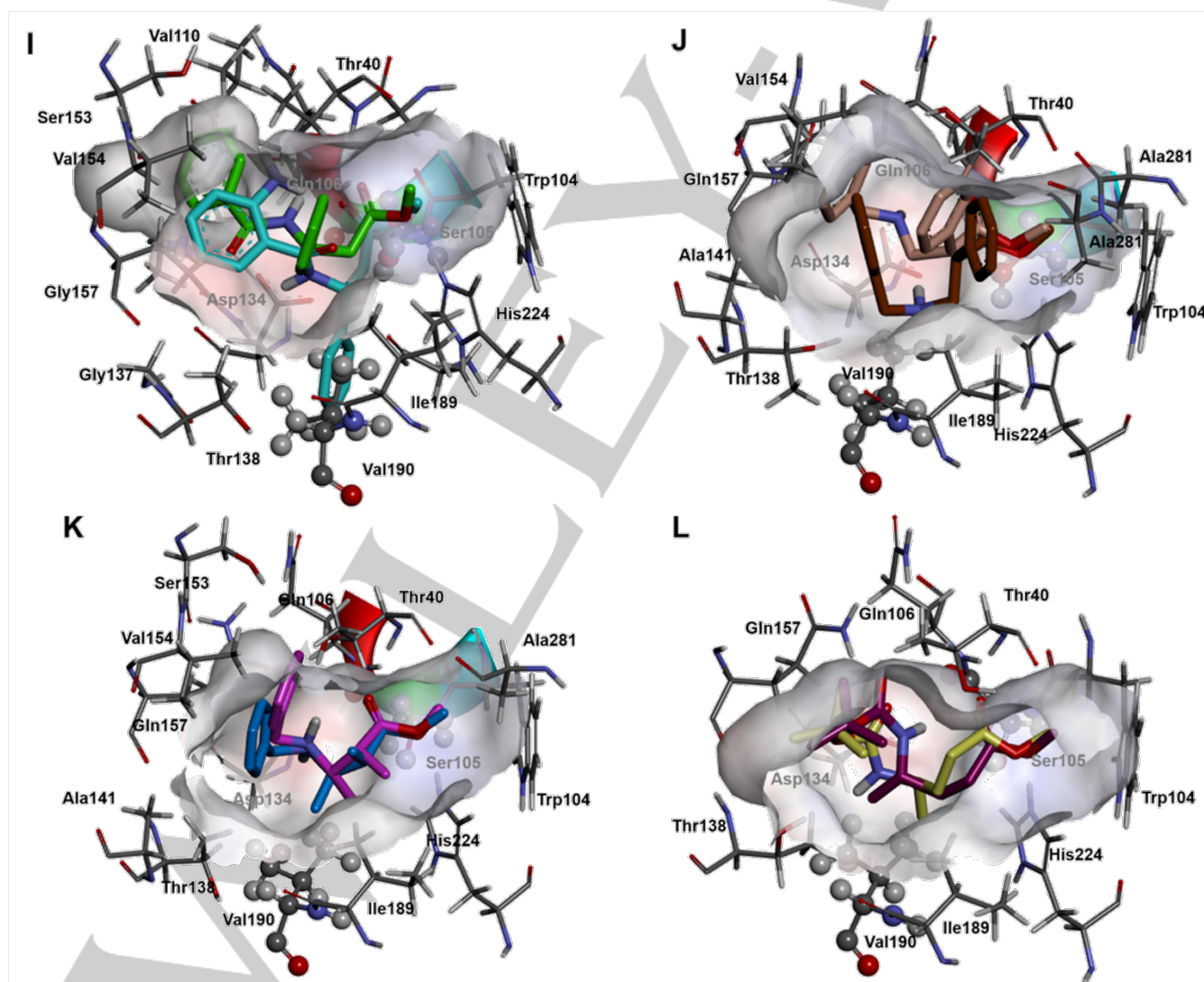


**Figure 4.** Steric repulsion effect at CaLB catalytic cavity: I, Substrates with  $\beta$  stereocenters Series 1; fast-reacting enantiomer (*S*)-**4i** in sticks (green), slow-reacting enantiomer (*R*)-**4i** in sticks (aqua). J, Substrates with  $\alpha$  stereocenters Series 2; fast-reacting enantiomer (*S*)-**4z** in sticks (beige), slow-reacting enantiomer (*R*)-**4z** in sticks (brown). K, Substrates with  $\beta$  and  $\alpha$  stereocenters Series 3; fast-reacting enantiomer *cis* (*2S,3R*)-**4x** in sticks (Blue), slow-reacting enantiomer (*2R,3S*)-**4x** in sticks (pink). L, Substrates with  $\gamma$  stereocenters Series 4; fast-reacting enantiomer (*S*)-**4a** in sticks (magenta), slow-reacting enantiomer (*R*)-**4a** in sticks (yellow). Exclusion residues Val190 and Ser105 in ball and sticks representation.

## FULL PAPER

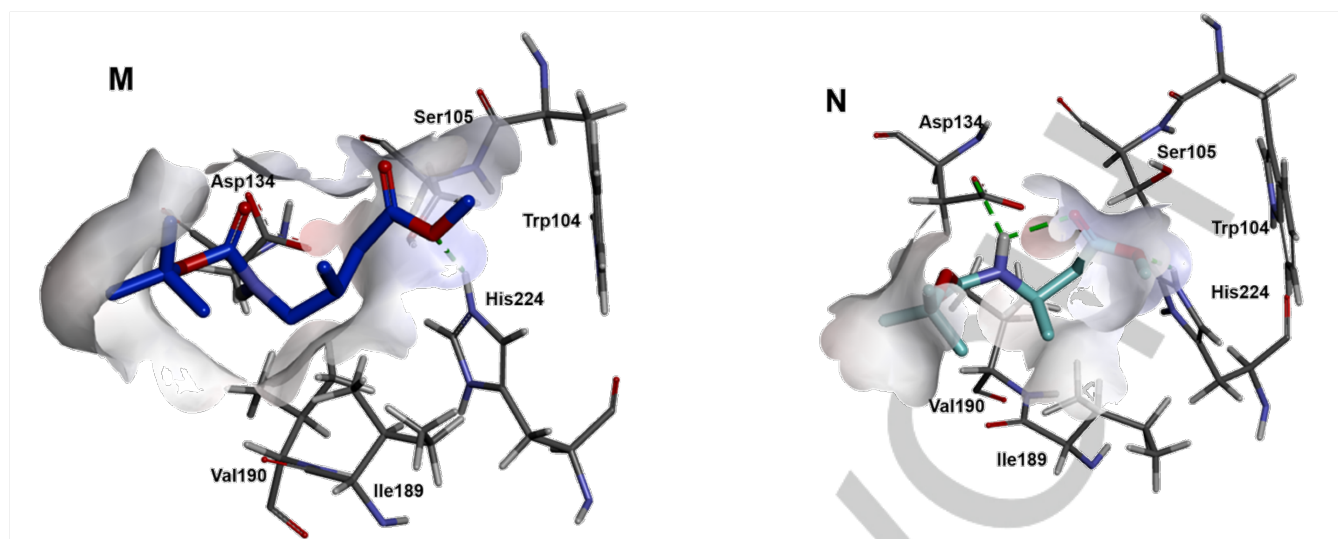


**Figure 5.** Amino position effect: **M**,  $\gamma^3$ -amino ester fast-reacting enantiomer (*R*)-**4b** in sticks (dark blue); **N**,  $\beta^3$ -amino ester fast-reacting enantiomer (*R*)-**4f** in sticks (light blue). Hydrogen bonds are displayed as green dashed lines

The docking analysis shows that the substituent at position  $\beta$  generates the greatest steric hindrance with the residues of Val190 and Ile189. Nevertheless, the  $\gamma^3$ -amino ester **4b** with a  $\beta$  stereocenter does not present steric repulsion in the catalytic cavity with Val 190 or Ile189 (**M** in Figure 5). These results are in agreement with experimental observation, that is the loss of selectivity of the  $\gamma^3$ -amino ester **4b** ( $E = 7.6$ ) relative to its analog **4f** ( $E = 458$ ).

#### Amino position effect

Although the steric repulsion effect explains the spatial requirement of the  $\beta^3$ - and  $\beta^{2,3}$ -amino esters with  $\beta$  stereocenters, it does not justify the loss of selectivity observed in the  $\gamma^3$ -amino ester with a  $\beta$  stereocenter (**4b**). Nevertheless, during the examination of the calculated conformations we detected that a stabilizing interaction by hydrogen bonding between Asp134 and the amino group is possible, and can play an important role during enantioselective resolutions. This interaction is well operative in most of the  $\beta$ -amino esters such as **4f** (Figure 5N). By contrast, such interaction is probably lost in the  $\gamma$ -amino esters, since they present greater conformational flexibility (Figure 5M).

#### Conclusions

In contrast with the results previously reported for the CalB-catalyzed enzymatic resolution of *N*-protected and *N*-benzylated  $\beta^3$ -amino methyl esters, the resolution of  $\gamma^3$ -amino methyl esters exhibited poor enantioselectivity. Based on the experimental and molecular docking results, two new regions were identified in the CalB catalytic cavity: (1) the sterically repulsive region composed of Val190 and Ile189 residues, which seem to be responsible for the high selectivity in the resolution of derivatives of carboxylic acids incorporating  $\beta$  stereocenters. This exclusion effect is not effective for derivatives of  $\beta$  and  $\gamma$  amino esters with  $\alpha$  and  $\gamma$  stereocenters, which helps explain the experimentally observed loss of selectivity. (2) The amino binding region interaction that is rather efficient with  $\beta$ -amino esters; however, the  $\gamma$ -aminoesters

show a broader conformational diversity, so this interaction is affected, which may be the reason for the loss of enantioselectivity for this class of esters.

#### Experimental Section

**General:** The lipase Novozym® 435 (Novozymes, Mexico) was used as the catalyst for all enzymatic reactions. Novozym® 435 is the commercially available form of the recombinant Lipase B from *Candida antarctica*, immobilized by adsorption in a hydrophobic microporous acrylic resin.<sup>[14e]</sup> Thin layer chromatography (TLC) was carried out on precoated silica gel 60 F<sub>254</sub>. Column chromatography was performed on Merck silica gel 60 (0.040-0.063 mm). <sup>1</sup>H and <sup>13</sup>C NMR spectra were recorded on Varian Gemini 200 MHz, Varian Mercury 400 MHz or Bruker 500 MHz equipments. Chemical  $\delta$  values (ppm) are reported relative to internal tetramethylsilane (TMS) reference ( $\delta = 0.0$  ppm) for determinations in CDCl<sub>3</sub> or calibrated against the residual impurity of CDCl<sub>3</sub> ( $\delta = 7.26$  ppm) and CD<sub>3</sub>OD ( $\delta = 3.31$  ppm). Gas Chromatography-Mass Spectrometry (GC-MS) was recorded on an Agilent GC system 6890 series coupled to an Agilent mass selective detector. Enantiomeric excesses for compounds **5a** and **7a** were determined by Chiral GC-MS with a SYCLOSIL-B column length 30 m, internal size 0.25 mm, film thickness 0.25  $\mu$ m, splitless, 120 °C at 0 min, 2 °C min<sup>-1</sup> to 180 °C by 1 min<sup>-1</sup>; retention times: (*R*)-**5a** and (*R*)-**7a** = 17.62 min; (*S*)-**5a** and (*S*)-**7a** = 17.77 min; (*R*)-**5b** and (*R*)-**7b** = 20.35 min; (*S*)-**5b** and (*S*)-**7b** = 20.50 min; (*R*)-**5c** and (*R*)-**7c** = 21.51 min; (*S*)-**5c** and (*S*)-**7c** = 21.66 min. All *N*-Boc protected  $\gamma$ -amino acids (**6a-c**) were converted into the corresponding methyl esters before their GC analysis. Optical rotations were measured by means of a Perkin-Elmer 341 polarimeter. Mass analyses were carried out by Liquid Chromatography-Mass Spectrometry (LC-MS) in an Agilent 6545 (LC-MS) spectrometer, by electrospray ionization and quadrupole time-of-flight (ESI-QTOF). Microwave Reactions were performed in sealed vessels in a monomode microwave CEM Discover apparatus.

**General procedure for the synthesis of methyl 4-nitro alkyl esters via microwave irradiation (GP1).** A solution of  $\alpha,\beta$ -unsaturated ester (**1a-c**) and the corresponding nitroalkane (**1d** or **1e**) were added to a glass microwave reaction vessel containing a stir bar. The vial was placed in an ice bath before the dropwise addition of the 1,1,3,3-Tetramethylguanidine (TMG) or 1,8-Diazabicyclo(5.4.0)undec-7-ene (DBU) as base with stirring. The reaction vessel was sealed and placed into the microwave cavity on

## FULL PAPER

“open vessel” mode, at the desired temperature and power conditions. Once the reaction was complete, the vessel was allowed to cool to ambient temperature. The crude mixture was purified by column chromatography.

**Methyl 4-nitropentanoate** [*rac*-**2a**] and **Dimethyl 4-methyl-4-nitroheptadionate** (**3a**). Prepared from methyl acrylate (**1a**, 1.72 g, 20 mmol), nitroethane (**1e**, 1.87 g, 25 mmol) and (TMG) (1.26 g, 0.55 eq). The microwave unit was programmed to 60 °C and a power of 50 watts for 5 min. After the reaction was completed, the vessel was cooled to below 50 °C using a flow of compressed air. The crude mixture was purified by column chromatography (hexane/EtOAc 90:10), afforded the products **2a** and **3a** as colorless oils, with yield of 65 % in 58:42 proportion respectively. Compound *rac*-**2a**: <sup>1</sup>H NMR (400 MHz, CDCl<sub>3</sub>) δ= 1.57 (d, *J* = 6.8 Hz, 3H, CH<sub>3</sub>CH); 2.05-2.14 (m, 1H, CHCH<sub>2A</sub>); 2.23-2.35 (m, 1H, CHCH<sub>2B</sub>); 2.38-2.47 (m, 2H, CH<sub>2</sub>CO); 3.70 (s, 3H, OCH<sub>3</sub>); 4.62-4.67 (m, 1H, NO<sub>2</sub>CH). <sup>13</sup>C NMR (100 MHz, CDCl<sub>3</sub>) δ= 19.5, 30.0, 30.1, 52.1, 82.6, 172.6. Compound **3a**: <sup>1</sup>H NMR (400 MHz, CDCl<sub>3</sub>) δ= 1.55 (s, 3H, CH<sub>3</sub>C); 2.12-2.23 (m, 2H, CH<sub>2A</sub>C); 2.27-2.43 (m, 6H, CH<sub>2B</sub>C+CH<sub>2</sub>); 3.69 (s, 6H, OCH<sub>3</sub>). <sup>13</sup>C NMR (100 MHz, CDCl<sub>3</sub>) δ= 21.9, 28.9, 34.3, 52.2, 89.8, 172.6. Spectral data <sup>1</sup>H and <sup>13</sup>C-NMR are consistent with the literature.<sup>[26]</sup>

**Methyl 3-methyl-4-nitrobutanoate** [*rac*-**2b**] and **Dimethyl 3,5-dimethyl-4-nitroheptadionate** (**3b**). Prepared from methyl crotonate (**1b**, 3.50 g, 35 mmol), nitromethane (**1d**, 5.34 g, 87.5 mmol), and DBU (0.26 g, 0.05 eq). The microwave unit was programmed to 60 °C and a power of 50 watts for 15 min. After the reaction was completed, the vessel was cooled to below 50 °C using a flow of compressed air. The crude mixture was purified by column chromatography (hexane/EtOAc 98:2 to 90:10), afforded the products *rac*-**2b** and **3b** as colorless oils, with yield of 58 % in a 98:2 proportion respectively. Compound *rac*-**2b**: <sup>1</sup>H NMR (200 MHz, CDCl<sub>3</sub>) δ= 1.10 (d, *J* = 6.8 Hz, 3H, CH<sub>3</sub>CH); 2.35 (dd, <sup>2</sup>*J* = 16.3 Hz, <sup>3</sup>*J* = 6.6 Hz, 1H, CH<sub>2A</sub>CO) 2.47 (dd, <sup>2</sup>*J* = 16.3 Hz, <sup>3</sup>*J* = 7.1 Hz, 1H, CH<sub>2B</sub>CO); 2.67-2.90 (m, 1H, CH); 3.69 (s, 3H, OCH<sub>3</sub>); 4.34 (dd, <sup>2</sup>*J* = 12.1 Hz, <sup>3</sup>*J* = 7 Hz, 1H, NO<sub>2</sub>CH<sub>2A</sub>) 4.48 (dd, <sup>2</sup>*J* = 12.1 Hz, <sup>3</sup>*J* = 6.3 Hz, 1H, NO<sub>2</sub>CH<sub>2B</sub>). <sup>13</sup>C NMR (50 MHz, CDCl<sub>3</sub>) δ= 17.3, 29.5, 37.7, 51.8, 80.3, 171.8. Spectral data <sup>1</sup>H and <sup>13</sup>C NMR are consistent with the literature.<sup>[26]</sup> Compound **3b** was obtained as inseparable mixture of diastereoisomers. See supplementary material.

**Methyl 2-methyl-4-nitrobutanoate** [*rac*-**2c**] and **Dimethyl 2,4-dimethyl-4-nitroheptadionate** (**3c**). Prepared from methyl methacrylate (**1c**, 2.00 g, 20 mmol), nitromethane (**1d**, 1.52 g, 25 mmol) and TMG (1.15 g, 0.5 eq). The microwave unit was programmed to 60 °C and a power of 50 watts for 20 min. After the reaction was completed, the vessel was cooled to below 50 °C using a flow of compressed air. The crude mixture was purified by column chromatography (hexane/EtOAc 98:2), afforded the products *rac*-**2c** and **3c** as colorless oils, with yield of 66 % in 65:35 proportion respectively. Compound *rac*-**2c**: <sup>1</sup>H NMR (400 MHz, CDCl<sub>3</sub>) δ= 1.19 (d, *J* = 7.1 Hz, 3H, CH<sub>3</sub>CH); 2.06-2.14 (m, 1H, CH<sub>2A</sub>CH); 2.23-2.32 (m, 1H, CH<sub>2B</sub>CH); 2.50-2.58 (m, 1H, CH<sub>3</sub>CH); 3.65 (s, 3H, OCH<sub>3</sub>); 4.35-4.46 (m, 2H, NO<sub>2</sub>CH<sub>2</sub>). <sup>13</sup>C NMR (100 MHz, CDCl<sub>3</sub>) δ= 17.1, 30.7, 36.6, 52.0, 73.5, 175.3. Compound **3c**: <sup>1</sup>H NMR (200 MHz, CDCl<sub>3</sub>) δ= 1.19 (d, *J* = 7.1 Hz, 6H, CH<sub>3</sub>CH); 1.91-2.19 (m, 4H, CHCH<sub>2</sub>CH); 2.35- 2.53 (m, 2H, CHCO); 3.69 (s, 6H, OCH<sub>3</sub>); 4.56-4.69 (m, 1H, NO<sub>2</sub>CH). <sup>13</sup>C NMR (50 MHz, CDCl<sub>3</sub>) δ= 18.0, 36.4, 37.7, 52.2, 85.6, 175.6. Spectral data <sup>1</sup>H and <sup>13</sup>C NMR are consistent with the literature.<sup>[26]</sup>

**General procedure for the synthesis of *N*-Boc protected  $\gamma$ -amino esters (GP2).** The hydrogenation reactions were carried out in a Shaker Hydrogenation Apparatus. A solution of nitro ester, Boc<sub>2</sub>O (1.1 eq) and Ni-Raney (10% mass) in MeOH (5 mL/mmol) was added to a hydrogenation flask. Reaction flask was placed into the hydrogenation apparatus and filled with H<sub>2</sub> to 60 psi, the reaction was monitored by TLC to observed disappearance of nitro ester to six hours of reaction time. The catalyst was filtered off and solvent evaporated under reduced pressure. The resulting crude product was purified on SiO<sub>2</sub> using hexane/EtOAc.

**Methyl 4-(*tert*-butoxycarbonyl)amino-pentanoate** [*rac*-**4a**]: Prepared from nitro ester *rac*-**2a** (0.50 g, 3.1 mmol), Boc<sub>2</sub>O (0.74 g, 1.1 eq) and Ni-

Raney (0.05 g, 10% mass) and 15.5 mL of MeOH according GP2. The crude mixture was purified by column chromatography (hexane/EtOAc 95:05) to give the product as a white solid, mp 24-25 °C, Yield: 75 %. R<sub>f</sub>= 0.44 (hexane/EtOAc, 70:30). <sup>1</sup>H NMR (200 MHz, CDCl<sub>3</sub>) δ= 1.14 (d, *J* = 6.6 Hz, 3H, CH<sub>3</sub>CH); 1.44 (s, 9H, [(CH<sub>3</sub>)<sub>3</sub>C]); 1.64-1.89 (m, 2H, CHCH<sub>2</sub>); 2.38 (t, *J* = 7.6 Hz, 2H, CH<sub>2</sub>CO); 3.68 (s, 4H, CH<sub>3</sub>CH+OCH<sub>3</sub>), 4.47 (br s, 1H, NH). <sup>13</sup>C NMR (50 MHz, CDCl<sub>3</sub>) δ= 21.5, 28.5, 31.0, 32.3, 46.4, 51.7, 79.3, 155.5, 174.1. Spectral data <sup>1</sup>H are consistent with the literature.<sup>[29]</sup> LC-HRMS (ESI-QTOF) calculated for [C<sub>11</sub>H<sub>21</sub>NO<sub>4</sub>]<sup>+</sup> requires 231.1471, found 231.1468.

**Methyl 4-(*tert*-butoxycarbonyl)amino-3-methylbutanoate** [*rac*-**4b**]: Prepared from nitro ester *rac*-**2b** (0.50 g, 3.9 mmol), Boc<sub>2</sub>O (0.74 g, 1.1 eq) and Ni-Raney (0.05 g, 10% mass) and 15.5 mL of MeOH according GP2. The crude mixture was purified by column chromatography (hexane/EtOAc 90:10) to give the product as a colorless oil Yield: 65 %. R<sub>f</sub>= 0.47 (hexane/EtOAc t, 70:30). <sup>1</sup>H NMR (200 MHz, CDCl<sub>3</sub>) δ= 0.96 (d, *J* = 6.5 Hz, 3H, CH<sub>3</sub>CH); 1.44 (s, 9H, [(CH<sub>3</sub>)<sub>3</sub>C]); 2.05-2.23 (m, 2H, CH<sub>2A</sub>CO+CH); 2.30-2.44 (m, 1H, CH<sub>2B</sub>CO); 3.05 (pseudo t, *J* = 5.8 Hz, 2H, CHCH<sub>2</sub>); 3.68 (s, 3H, OCH<sub>3</sub>); 4.74 (br s, 1H, NH). <sup>13</sup>C NMR (50 MHz, CDCl<sub>3</sub>) δ= 17.9, 28.6, 31.4, 39.0, 46.2, 51.7, 79.4, 156.2, 173.5. Spectral data <sup>1</sup>H and <sup>13</sup>C NMR are consistent with the literature.<sup>[30]</sup> LC-HRMS (ESI-QTOF) calculated for [C<sub>11</sub>H<sub>21</sub>NO<sub>4</sub>]<sup>+</sup> requires 231.1471, found 231.147.

**Methyl 4-(*tert*-butoxycarbonyl)amino-2-methylbutanoate** [*rac*-**4c**]: Prepared from nitro ester *rac*-**2c** (0.50 g, 3.1 mmol), Boc<sub>2</sub>O (0.74 g, 1.1 eq), Ni-Raney (0.05 g, 10% mass) and 15.5 mL of MeOH according GP2. The crude mixture was purified by column chromatography (hexane/EtOAc 90:10) to give the product as a colorless oil Yield: 60 %. R<sub>f</sub>= 0.47 (hexane/EtOAc, 70:30). <sup>1</sup>H NMR (500 MHz, CDCl<sub>3</sub>) δ= 1.18 (d, *J* = 7.1 Hz, 3H, CH<sub>3</sub>CH); 1.44 (s, 9H, [(CH<sub>3</sub>)<sub>3</sub>C]); 1.59-1.67 (m, 1H, CH<sub>2A</sub>CH); 1.84 (m, 1H, CH<sub>2B</sub>CH); 2.51 (m, 1H, CH<sub>3</sub>CH); 3.15 (m, 2H, CH<sub>2</sub>NH); 3.68 (s, 3H, OCH<sub>3</sub>); 4.72 (br s, 1H, NH). <sup>13</sup>C NMR (50 MHz, CDCl<sub>3</sub>) δ= 17.2, 28.5, 33.9, 37.2, 38.7, 51.8, 79.3, 156.0, 176.9. Spectral data <sup>1</sup>H and <sup>13</sup>C are consistent with the literature.<sup>[31]</sup> LC-HRMS (ESI-QTOF) calculated for [C<sub>11</sub>H<sub>21</sub>NO<sub>4</sub>]<sup>+</sup> requires 231.1471, found 231.1468.

## Enzymatic reactions

**General procedure for the enzymatic hydrolysis of *N*-Boc protected  $\gamma$ -amino esters (GP3).** Enzymatic hydrolysis reactions were carried out in sealed glass vials. The reactions consisted in the preparation of solution of the corresponding  $\gamma$ -amino esters *rac*-**4a-c** (0.20 g, 0.86 mmol), 20 mg mL<sup>-1</sup> of CaLB (Novozym® 435), 2 equivalents of water (31  $\mu$ L) in 4.32 mL of anhydrous 2M2B solvent (0.2 M). The reaction mixtures were stirred in a thermostated water bath at 45 °C or at room temperature. At the end of reaction the enzyme was filtered off and washed with DCM. The solvent was evaporated in vacuum. The proportions of **5a-c** and **6a-c** in the reaction crude were determined by <sup>1</sup>H NMR. The products were purified by filtration over SO<sub>2</sub> using hexane/EtOAc (90:10 to 60:40).

**(*R*)-(+)-Methyl 4-(*tert*-butoxycarbonyl)amino-pentanoate** [(*R*)-(+)-**5a**]. Recovered ester: 52%. White solid, mp 24-25 °C, [ $\alpha$ ]<sub>D</sub><sup>20</sup> = +2 (c 1, CHCl<sub>3</sub>); 60.3 % ee. <sup>1</sup>H and <sup>13</sup>C NMR data are in accordance with those reported for **4a**.<sup>[29]</sup>

**(*S*)-(+)-Methyl 4-(*tert*-butoxycarbonyl)amino-3-methylbutanoate** [(*S*)-(+)-**5b**]. Recovered ester: 69 %. Colorless oil. [ $\alpha$ ]<sub>D</sub><sup>20</sup> = +0.16 (c 1, CHCl<sub>3</sub>); 30.9 % ee. <sup>1</sup>H and <sup>13</sup>C NMR data are in accordance with those reported for **4b**.<sup>[30]</sup>

**(*S*)-(+)-Methyl 4-(*tert*-butoxycarbonyl)amino-2-methylbutanoate** [(*S*)-(+)-**5c**]. Recovered ester: 69 %. Colorless oil. [ $\alpha$ ]<sub>D</sub><sup>20</sup> = +3.1 (c 1, CHCl<sub>3</sub>); 16.2 % ee. <sup>1</sup>H and <sup>13</sup>C NMR data are in accordance with those reported for **4c**.<sup>[31]</sup>

**(*S*)-(+)-4-(*tert*-Butoxycarbonyl)amino-pentanoic acid** [(*S*)-(+)-**6a**]. Yield: 48 %. White solid, mp 78-79 °C [lit.<sup>[32]</sup> (*S*)-**6a**: 75-78 °C; [ $\alpha$ ]<sub>D</sub><sup>20</sup> = +3.5

## FULL PAPER

(*c* 1.0, CHCl<sub>3</sub>); 64.1 % *ee* {lit.<sup>[8b]</sup> (*S*)-**6a**; [ $\alpha$ ]<sub>D</sub><sup>20</sup> = +2.4 (*c* 4, EtOH)}. <sup>1</sup>H NMR (200 MHz, CDCl<sub>3</sub>)  $\delta$  = 1.13 (d, *J* = 6.6 Hz, 3H, CH<sub>3</sub>CH); 1.42 (s, 9H, [(CH<sub>3</sub>)<sub>3</sub>C]); 1.58-1.88 (m, 2H, CHCH<sub>2</sub>); 2.38 (t, *J* = 7.4 Hz, 2H, CH<sub>2</sub>CO); 3.72 (m, 1H, CHCH<sub>3</sub>), 4.47 (br s, NH), 9.46 (br s, 1H, OH). <sup>13</sup>C NMR (50 MHz, CDCl<sub>3</sub>)  $\delta$  = 21.5, 28.6, 31.2, 32.3, 46.4, 79.7, 155.9, 178.6. Spectral data <sup>1</sup>H and <sup>13</sup>C NMR are consistent with the literature.<sup>[32]</sup> LC-HRMS (ESI-QTOF) calculated for [C<sub>10</sub>H<sub>19</sub>NO<sub>4</sub>]<sup>+</sup> requires 217.1314, found 217.1326.

**(*R*)-(+)-4-(tert-Butoxycarbonyl)amino-3-methylbutanoic acid** [(*R*)-(+)-**6b**]. Yield: 31 %. Colorless resin. [ $\alpha$ ]<sub>D</sub><sup>20</sup> = +2.7 (*c* 1, CHCl<sub>3</sub>); 70 % *ee* {lit.<sup>[28]</sup> (*R*)-**6b**; [ $\alpha$ ]<sub>D</sub><sup>20</sup> = +4.3 (*c* 1.05, CHCl<sub>3</sub>)}, <sup>1</sup>H NMR (200 MHz, CD<sub>3</sub>OD)  $\delta$  = 0.94 (d, *J* = 6.4 Hz, 3H, CH<sub>3</sub>CH); 1.44 (s, 9H, [(CH<sub>3</sub>)<sub>3</sub>C]); 1.98-2.16 (m, 2H, CH<sub>2</sub>CO + CH); 2.29-2.43 (m, 1H, CH<sub>2</sub>CO); 2.96 (d, *J* = 6.4 Hz, 2H, CH<sub>2</sub>NH). <sup>13</sup>C NMR (50 MHz, CD<sub>3</sub>OD)  $\delta$  = 17.8, 28.8, 32.4, 39.8, 46.9, 79.9, 158.6, 176.6. Spectral data <sup>1</sup>H and <sup>13</sup>C NMR are consistent with the literature.<sup>[28]</sup> LC-HRMS (ESI-QTOF) calculated for [C<sub>10</sub>H<sub>19</sub>NO<sub>4</sub>]<sup>+</sup> requires 217.1314, found 217.1324.

**(*R*)-(-)-4-(tert-Butoxycarbonyl)amino-2-methylbutanoic acid** [(*R*)-(-)-**6c**]. Yield: 31 %. Colorless resin. [ $\alpha$ ]<sub>D</sub><sup>20</sup> = -7.6 (*c* 1, CHCl<sub>3</sub>); 35.6 % *ee* {lit.<sup>[28]</sup> (*R*)-[ $\alpha$ ]<sub>D</sub><sup>20</sup> = -15.5 (*c* 1.04, CHCl<sub>3</sub>)}, <sup>1</sup>H NMR (200 MHz, CD<sub>3</sub>OD)  $\delta$  = 1.16 (d, *J* = 7 Hz, 3H, CH<sub>3</sub>CH); 1.43 (s, 9H, [(CH<sub>3</sub>)<sub>3</sub>C]); 1.41-1.62 (m, 1H, CHCH<sub>2A</sub>); 1.74-1.92 (m, 1H, CHCH<sub>2B</sub>); 2.36-2.53 (m, 1H, CH); 3.08 (t, *J* = 7.2 Hz, 2H, CH<sub>2</sub>NH). <sup>13</sup>C NMR (50 MHz, CD<sub>3</sub>OD)  $\delta$  = 17.5, 28.8, 34.8, 38.1, 39.4, 79.9, 158.5, 180.1. Spectral data <sup>1</sup>H and <sup>13</sup>C NMR are consistent with the literature.<sup>[28]</sup> LC-HRMS (ESI-QTOF) calculated for [C<sub>10</sub>H<sub>19</sub>NO<sub>4</sub>]<sup>+</sup> requires 217.1314, found 217.1323.

**General procedure for the esterification of *N*-Boc protected  $\gamma$ -amino acids (GP4).** To a solution of *N*-Boc-Protected  $\gamma$ -amino acid in MeOH/toluene 3:2 (8 mL mmol<sup>-1</sup>) was placed in an ice bath then was added 2 eq of TMS-CHN<sub>2</sub> (2 M in hexanes), the reaction mixture was stirred overnight. After the reaction was completed, the solvent was evaporated in vacuum and the crude mixture was purified by column chromatography to give the products as colorless oils.

**(*S*)-(-)-Methyl 4-(tert-butoxycarbonyl)amino-pentanoate** [(*S*)-(-)-**7a**]: Prepared from **6a** (0.06 g, 0.27 mmol), MeOH/toluene 3:2 (2.2 mL) and TMS-CHN<sub>2</sub> 2M in hexanes (0.27 mL, 2 eq) according GP4. The crude mixture was purified by column chromatography (hexane/EtOAc 90:10 to 40:60). Yield: 92 %. [ $\alpha$ ]<sub>D</sub><sup>20</sup> = -2.3 (*c* 0.68, CHCl<sub>3</sub>); 64.1 % *ee*. White solid. <sup>1</sup>H and <sup>13</sup>C NMR data are in accordance with those reported for **4a**.<sup>[29]</sup>

**(*R*)-(-)-Methyl 4-(tert-butoxycarbonyl)amino-3-methylbutanoate** [(*R*)-(-)-**7b**]: Prepared from **6b** (0.09 g, 0.08 mmol), MeOH/toluene 3:2 (0.680 mL) and TMS-CHN<sub>2</sub> 2M in hexanes (0.085 mL, 2 eq) according GP4. The crude mixture was purified by column chromatography (hexane/EtOAc 90:10 to 40:60). Yield: 71 %. Colorless oil. [ $\alpha$ ]<sub>D</sub><sup>20</sup> = -0.96 (*c* 1.04, CHCl<sub>3</sub>); 70 % *ee*. <sup>1</sup>H and <sup>13</sup>C NMR data are in accordance with those reported for **4b**.<sup>[30]</sup>

**(*R*)-(-)-Methyl 4-(tert-butoxycarbonyl)amino-2-methylbutanoate** [(*R*)-(-)-**7c**]: Prepared from **6c** (0.03 g, 1.33 mmol), MeOH/toluene 3:2 (1 mL) and TMS-CHN<sub>2</sub> 2M in hexanes (0.13 mL, 2 eq) according GP4. The crude mixture was purified by column chromatography (hexane/EtOAc 90:10 to 40:60). Yield: 77 %. Colorless oil. [ $\alpha$ ]<sub>D</sub><sup>20</sup> = -9.9 (*c* 1.04, CHCl<sub>3</sub>); 35.6 % *ee*. <sup>1</sup>H and <sup>13</sup>C NMR data are in accordance with those reported for **4c**.<sup>[31]</sup>

**(*R*)-(+)-5-Methyl-2-pyrrolidinone** [(*R*)-(+)-**8a**]: To a solution of [(*R*)-(+)-**5a** (0.18 g, 0.77 mmol) in DCM was added a solution of TFA/DCM 1:2 (5.4 mL, 1 mL TFA / 100 mg sample); the reaction was monitored by TLC to observed disappearance of **5a**, the reaction mixture was diluted with hexane to drag the TFA then was evaporated under reducer pressure. The crude mixture was then refluxed in toluene to obtain **8a** as colorless oil. Yield: 11 %. [ $\alpha$ ]<sub>D</sub><sup>20</sup> = +4 (*c* 1, EtOH); {lit.<sup>[27]</sup> (*R*); [ $\alpha$ ]<sub>D</sub><sup>20</sup> = +17.2 (*c* 1.02, EtOH)}; <sup>1</sup>H NMR (200 MHz, CDCl<sub>3</sub>)  $\delta$  = 1.22 (d, *J* = 6.3 Hz, 3H, CH<sub>3</sub>CH); 1.56-1.73 (m, 1H, CH<sub>2A</sub>CH); 2.17-2.4 (m, 3H, CH<sub>2B</sub>CH+CH<sub>2</sub>CO); 3.70-3.86 (m, 1H, CH<sub>3</sub>CH); 6.27 (br s, 1H, NH); <sup>13</sup>C NMR (50 MHz, CDCl<sub>3</sub>)  $\delta$  =

178.6, 50.4, 30.7, 29.4, 22.3. Spectral data <sup>1</sup>H and <sup>13</sup>C NMR are consistent with the literature.<sup>[27]</sup>

**Computational methods***Ligands preparation*

**rac-4a-z** Structures were constructed in Spartan'18;<sup>[33]</sup> these molecules were then submitted to a conformational analysis within the molecular mechanics level theory employing the MMFF force field. The structures of all the minimum energy conformers were fully optimized, without symmetry restrictions, within the density functional theory (DFT) using the B3LYP hybrid functional and the 6-31\*G basis set. All vibrational frequencies were positive, ensuring that all structures were in a minimum of the potential energy surface. The ligands for the molecular docking were used with Mulliken charges.

*CaLB structural analysis*

All molecular docking calculations were carried out in Molegro Virtual Docker (MVD).<sup>[34]</sup> The X-ray structure of CaLB used for molecular docking was 1LBS PDB code with a phosphonate inhibitor in the catalytic cavity. 1LBS was used as the monomer, all the water molecules as well as the *N*-acetyl-d-glucosamine molecule were removed. His224 was diprotonated to ensure the formation of the hydrogen bond between His224 and the oxygen of the ester. The variation of the tertiary structure in 1LBS was determined using Visual Molecular Dynamics (VMD),<sup>[35]</sup> by means of a structural alignment taking as reference the structure of CaLB of higher resolution (1.55 Å) with PDB code: 1TCA, but without ligand in the cavity. It was determined that the main chain of the protein in the 1LBS structure does not undergo important modifications caused by the inductive effect of the ligand in its cavity (RMSD = 0.33 Å).

*Molecular Docking*

The molecular Docking calculations were performed in Molegro Virtual Docker.<sup>[34]</sup> Dockings were done at the phosphonate inhibitor binding site (cavity volume is 194.05 Å<sup>3</sup>). The side chains of the amino acid residues at 6 Å from the ligand were made flexible (34 amino acids). The search algorithm was MolDock SE (Simplex Evolution) with the following parameters: a total of 15 runs with a maximum of 2,000 iterations, using a population of 50 individuals, 2,000 minimization steps for each flexible residue, and 2,000 global minimization steps per run. The calculated conformations were evaluated in terms of the enzyme-substrate interaction energy, through the scoring function used by Molegro® (MolDoc Score), which is given in kcal/mol and is the sum of the enzyme-ligand intermolecular energy and the contribution of the internal energy of the ligand.

The scoring function to calculate the docking energy value was the MolDock Score [GRID]. It was set on a 0.2 Å grid and attached the 10 Å radius search sphere around the cavity. For the energy analysis of the ligand, internal electrostatic interactions, internal hydrogen bonds and sp<sup>2</sup>-sp<sup>2</sup> deformations were considered.

The experimental ligand (catalytically non-productive conformation) in the 1LBS, was reproduced by a calculated conformation with a value of RMSD = 1.1 Å. Additionally, a catalytically productive calculated conformation was obtained, in which we can observe the ethoxy of the ligand oriented towards the nucleophile pocket, forming a weak hydrogen bond with the His224 residue.

A docking template was created considering the structural characteristics of the catalytically productive calculated conformation such as positive and negative charges, hydrogen bond donors and acceptors, and steric factors.

All the structures of docking of this work were made with Discovery Studio Visualizer.<sup>[36]</sup>

**Acknowledgements**

This research was supported by PAPIIT-UNAM (grant PAPIIT-IT200220). We are also indebted to CONACYT, Mexico for

## FULL PAPER

financial support via grants CB2015/256653, 220945 and A1-S-44097, and to fund SEP-CINVESTAV for financial support via grant 126. M.A.O-R thanks to CONACyT for the graduate scholarship 266948. M.A.O-R. and R.S.R-H. thanks to Mario A. Leyva-Peralta from University of Sonora and Zeferino Gómez Sandoval from University of Colima for allowing access to their software resources. We thank to Maria G. Medina Pintor for technical assistance. We are also grateful to the reviewers for many useful comments.

**Keywords:**  $\gamma$ -Amino methyl esters • Biocatalysis • Enantiodiscrimination • Kinetic resolution • Molecular Docking

## References:

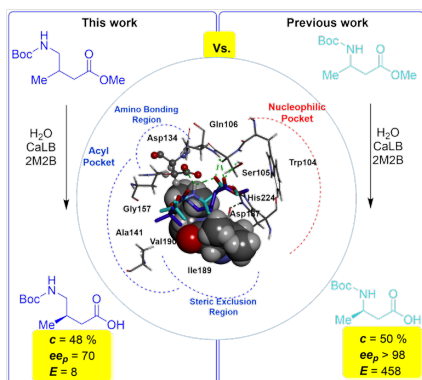
- [1] a) D. C. Blakemore, L. Castro, I. Churcher, D. C. Rees, A. W. Thomas, D. M. Wilson, A. Wood, *Nat. Chem.* **2018**, *10*, 383–394; b) X. Wang, *Nat. Catal.* **2019**, *2*, 98–102.
- [2] J. Gal, in *Chirality in Drug Research, Vol. 33* (Eds: E. Francotte, W. Lindner), Wiley-VCH, Weinheim, **2006**, pp. 1–26.
- [3] a) L. Kiss, E. Forró, F. Fülöp in *Amino Acids, Peptides and Proteins in Organic Chemistry, Vol 1* (Eds: A. B. Hughes), Wiley-VCH, Weinheim, **2009**, pp. 367–409. b) E. Juaristi in *Enantioselective Synthesis of  $\beta$ -Amino acids, 2nd ed.* (Eds: E. Juaristi, V. A. Soloshonok), Wiley-VCH, New York, **2005**, pp. 1–17.
- [4] N. M. Maier, W. Lindner in *Chirality in Drug Research, Vol. 33* (Eds: E. Francotte, W. Lindner), Wiley-VCH, Weinheim, **2006**, pp. 189–260.
- [5] a) G. F. Breen, *Tetrahedron: Asymmetry* **2004**, *15*, 1427–1430. b) V. Gotor-Fernández, E. Busto, V. Gotor, *Adv. Synth. Catal.* **2006**, *348*, 797–812. c) H. Sun, H. Zhang, E. L. Ang, H. Zhao, *Bioorg. Med. Chem.* **2018**, *26*, 1275–1284.
- [6] a) E. Forró, F. Fülöp, *Curr. Med. Chem.* **2012**, *19*, 6178–6187. b) A. Liljeblad; L. T. Kanerva, *Tetrahedron* **2006**, *62*, 5831–5854. c) R. Singh, R. Vince, *Chem. Rev.* **2012**, *112*, 4642–4686. d) S. Shahmohammadi, F. Fülöp, E. Forró, *Molecules* **2020**, *25*, 5990. e) E. Forró, Z. Galla, F. Fülöp, *Eur. J. Org. Chem.* **2016**, 2647–2652. f) Z. Galla, F. Beke, E. Forró, F. Fülöp, *J. Mol. Catal. B: Enzym.* **2016**, *123*, 107–112. g) E. Forró, L. Kiss, J. Árvá, F. Fülöp, *Molecules* **2017**, *22*, 2211. h) M. Rodríguez-Mata, E. García-Urdiales, V. Gotor-Fernández, V. Gotor, *Adv. Synth. Catal.* **2010**, *352*, 395–406.
- [7] F. Fülöp, *Chem. Rev.* **2001**, *101*, 2181–2204.
- [8] a) D. Seebach, A. K. Beck, S. Capone, G. Deniau, U. Grošelj, E. Zass, *Synthesis*, **2009**, 1–32. b) T. Hintermann, K. Gademann, B. Jaun, D. Seebach, *Helv. Chim. Acta.* **1998**, *81*, 983–1002. c) S. Hanessian, X. Luo, R. Schaum, *Tetrahedron Lett.* **1999**, *40*, 4925–4929. d) D. Seebach, T. Kimmmerlin, R. Šebesta, M. A. Campo, A. K. Beck, *Tetrahedron* **2004**, *60*, 7455–7506.
- [9] a) J. S. Bryans, D. J. Wustrow, *Med. Res. Rev.* **1999**, *19*, 149–177. b) W. Froestl, *Future Med. Chem.* **2011**, *3*, 163–175. c) K. Gajcy, S. Lochynski, T. Librowski, *Curr. Med. Chem.* **2010**, *17*, 2338–2347. d) H. R. Olpe, H. Demiéville, V. Baltzer, W. L. Bencze, W. P. Koella, P. Wolf, H. L. Haas, *Eur. J. Pharmacol.* **1978**, *52*, 133–136. e) G. H. Fromm, C. F. Terrence, A. S. Chattha, J. D. Glass, *Arch. Neurol.* **1980**, *37*, 768–771.
- [10] a) S. Lotarski, H. Hain, J. Peterson, S. Galvin, B. Strenkowski, S. Donevan, J. Offord, *Epilepsy Res.* **2014**, *108*, 833–842. b) D. E. Feltnner, J. G. Crockatt, S. J. Dubovsky, C. K. Cohn, R. K. Shrivastava, S. D. Targum, M. Liu-Dumaw, C. M. Carter, A. C. Pande, *J. Clin. Psychopharmacol.* **2003**, *23*, 240–249. c) R. Matsuzawa, T. Fujiwara, K. Nemoto, T. Fukushima, S. Yamaguchi, K. Akagawa, Y. Hori, *Neurosci. Lett.* **2014**, *558*, 186–191.
- [11] a) E. Juaristi, V. M. Gutiérrez-García, H. López-Ruiz, in *Enantioselective Synthesis of  $\beta$ -Amino acids, 2nd ed.* (Eds: E. Juaristi, V. A. Soloshonok), Wiley-VCH: New York, **2005**, pp. 159–180. b) Y. Bandala, E. Juaristi, in *Amino Acids, Peptides and Proteins in Organic Chemistry, Vol 1* (Eds: A. B. Hughes), Wiley-VCH, Weinheim, **2009**, pp. 291–366. c) P. Ramesh, D. Suman, K. S. N. Reddy, *Synthesis* **2018**, *50*, 211–226.
- [12] a) E. Forró, F. Fülöp, *Eur. J. Org. Chem.* **2008**, 5263–5268. b) F. Felluga, G. Pitacco, E. Valentin, C. D. Venneri, *Tetrahedron: Asymmetry* **2008**, *19*, 945–955.
- [13] a) K. Hult, P. Berglund, *Curr. Opin. Biotechnol.* **2003**, *14*, 395–400. b) M. T. Reetz, *J. Am. Chem. Soc.* **2013**, *135*, 12480–12496. c) T. Itoh, U. Hanefeld, *Green Chem.* **2017**, *19*, 331–332. d) J. Albarrán-Velo, D. González-Martínez, V. Gotor-Fernández, *Biocatal. Biotransform.* **2017**, *36*, 102–130. e) U. T. Bornscheuer, R. J. Kazlauskas, *Angew. Chem. Int. Ed.* **2004**, *43*, 6032–6040. f) E. Busto, V. Gotor-Fernández, V. Gotor, *Chem. Soc. Rev.* **2010**, *39*, 4504–4523. g) M. S. Humble, P. Berglund, *Eur. J. Org. Chem.* **2011**, 3391–340. h) M. Kapoor, M. N. Gupta, *Process Biochem.* **2012**, *47*, 555–569. i) Z. Guan, L.-Y. Li, Y.-H. He, *RSC Adv.* **2015**, *5*, 16801–16814.
- [14] a) E. M. Anderson, K. M. Larsson, O. Kirk, *Biocatal. Biotransform.* **1998**, *16*, 181–204. b) Q. Wu, P. Soni, M. T. Reetz, *J. Am. Chem. Soc.* **2013**, *135*, 1872–1881. c) F. Haefner, T. Norin, *Chem. Pharm. Bull.* **1999**, *47*, 591–600. d) O. Kirk, M. W. Christensen, *Org. Proc. Res. Dev.* **2002**, *6*, 446–451. e) C. Ortiz, M. L. Ferreira, O. Barbosa, J. C. S. dos Santos, R. C. Rodrigues, Á. Berenguer-Murcia, L. E. Briand, R. Fernandez-Lafuente, *Catal. Sci. Technol.* **2019**, *9*, 2380–2420.
- [15] a) M. Pérez-Venegas, A. M. Rodríguez-Treviño, E. Juaristi, *ChemCatChem* **2020**, *12*, 1782–1788. b) M. Pérez-Venegas, E. Juaristi, *ACS Sust. Chem. Eng.* **2020**, *8*, 8881–8893. c) P. Borowiecki, D. Paprocki, M. Dranka, *Beilstein J. Org. Chem.* **2014**, *10*, 3038–3055. d) P. Borowiecki, D. Paprocki, A. Dudzik, J. Plenkiewicz, *J. Org. Chem.* **2016**, *81*, 380–395. e) P. Borowiecki, B. Zdun, M. Dranka, *Mol. Catal.* **2021**, *504*, 111451. f) P. Borowiecki, M. Młynek, M. Dranka, *Bioorg. Chem.* **2021**, *106*, 104448.
- [16] J.-H. Jung, D.-H. Yoon, P. Kang, W. K. Lee, H. Eum H.-J. Ha, *Org. Biomol. Chem.* **2013**, *11*, 3635–3641.
- [17] a) K. P. Dhake, P. J. Tambade, R. S. Singhal, B. M. Bhanage, *Tetrahedron Lett.* **2010**, *51*, 4455–4458. c) O. Torre, I. Alfonso, V. Gotor, *Chem. Commun.* **2004**, *4*, 1724–1725. d) M. A. Ortega-Rojas, J. D. Rivera-Ramírez, C. G. Ávila-Ortiz, E. Juaristi, F. González-Muñoz, E. Castillo, J. Escalante, *Molecules* **2017**, *22*, 2189. e) J. D. Rivera-Ramírez, J. Escalante, A. López-Munguía, A. Marty, E. Castillo, *J. Mol. Catal. B: Enzym.* **2015**, *112*, 76–82. f) J. Priego, C. Ortiz-Nava, M. Carrillo-Morales, A. López-Munguía, J. Escalante, E. Castillo, *Tetrahedron* **2009**, *65*, 536–539.
- [18] a) H. Ismail, R. M. Lau, L. M. van Langen, F. van Rantwijk, V. K. Švedas, R. A. Sheldon, *Green Chem.* **2008**, *10*, 415–418. b) P. Braiuca, K. Lorena, V. Ferrario, C. Ebert, L. Gardossi, *Adv. Synth. Catal.* **2009**, *351*, 1293–1302. c) E. García-Urdiales, F. Rebollo, V. Gotor, *Adv. Synth. Catal.* **2001**, *343*, 646–654. d) M. Pérez-Venegas, E. Juaristi, *Tetrahedron*, **2018**, *74*, 6453–6458. e) V. Gotor, in *Enzymes in Action Green Solutions for Chemical Problems, Vol 33* (Eds: B. Zwanenburg, M. Mikolajczyk, P. Kielbasiński), Springer, Dordrecht, **2000**, pp. 117–132. f) A. Torres-Gavilán, J. Escalante, I. Regla, A. López-Munguía, E. Castillo, *Tetrahedron: Asymmetry*, **2007**, *18*, 2621–2624. g) M. Nechab, N. Azzi, N. Vanthuyne, M. Bertrand, S. Gastaldi, G. Gil, *J. Org. Chem.* **2007**, *72*, 6918–6923. h) H. Lundberg, F. Tinnis, N. Selander, H. Adolfsson, *Chem. Soc. Rev.* **2014**, *43*, 2714–2742. i) F. Uthoff, A. Reimer, A. Liese, H. Gröger, *Sust. Chem. Pharm.* **2017**, *5*, 42–45. j) M. R. Petchey, G. Grogan, *Adv. Synth. Catal.* **2019**, *361*, 3895–3914. k) F. Uthoff, J. Löwe, C. Harms, K. Donsbach, H. Gröger, *J. Org. Chem.* **2019**, *84*, 4856–4866. l) R. N. Lima, C. S. dos Anjos, E. V. M. Orozco, A. L. M. Porto, *Mol. Catal.* **2019**, *466*, 75–105.
- [19] a) J. G. Hernández, M. Frings, C. Bolm, *ChemCatChem* **2016**, *8*, 1769–1772. b) N. Braia, M. Merabet-Khelassi, L. Aribi-Zouieouche, *Chirality* **2018**, *30*, 1312–1320. c) C. Orrenius, F. Haefner, D. Rotticci, T. Norin, K. Hult, *Biocatal. Biotransform.* **1998**, *16*, 1–15. c) P. Borowiecki, M. Dranka, Z. Ochal, *Eur. J. Org. Chem.* **2017**, 5378–5390. d) F. H. Blindheim, M. B. Hansen, S. Evjen, W. Zhu, E. E. Jacobsen, *Catalysts* **2018**, *8*, 516. e) T. d. S. Fonseca, L. D. Lima, M. d. C. F. de Oliveira, T. L. G. de Lemos, D. Zampieri, F. Molinari, M. C. de Mattos, *Eur. J. Org. Chem.* **2018**, 2110–2116. f) Q.-Y. Chen, P. R. Chaturvedi, H. Luesch, *Org. Proc. Res. Dev.* **2018**, *22*, 190–199. g) P. Borowiecki, M. Dranka, *Bioorg. Chem.* **2019**, *93*, 102754. h) D. Rotticci, F. Haefner, C. Orrenius, T. Norin, Karl Hult, *J. Mol. Catal. B: Enzym.* **1998**, *5*, 267–272.

## FULL PAPER

- [20] J. Uppenberg, N. Öhrner, M. Norin, K. Hult, G. J. Kleywegt, S. Patkar, V. Waagen, T. Anthonsen, T. A. Jones, *Biochemistry* **1995**, *34*, 16838–16851.
- [21] a) E. García-Urdiales, N. Rios-Lombardia, J. Mangas-Sánchez, V. Gotor Fernández, V. Gotor, *ChemBioChem* **2009**, *10*, 1830–1838. b) W. Li, B. Yang, Y. Wang, D. Wei, C. Whiteley, X. Wang, *J. Mol. Catal. B: Enzym.* **2009**, *57*, 299–303. c) K. Swiderek, S. Martí, V. Moliner, *ACS Catal.* **2014**, *4*, 426–434. d) P. B. Juhl, P. Trodler, S. Tyagi, J. Pleiss, *BMC Structural Biol.* **2009**, *9*, 39. e) M. S. S. Googheri, M. R. Housaindokht, H. Sabzyan, *J. Mol. Graph. Modell.* **2014**, *54*, 131–140. f) J. Gu, J. Liu, H. Yu, *J. Mol. Catal. B: Enzym.* **2011**, *72*, 238–247. g) J.-W. Shen, J.-M. Qi, X.-J. Zhang, Z.-Q. Liu, Y.-G. Zheng, *Catal. Sci. Technol.* **2018**, *8*, 4718–4725. h) C. Trapp, K. Barková, M. J. Pecyna, C. Herrmann, A. Fuchs, D. Greif, M. Hofrichter, *Mol. Catal.* **2021**, *509*, 111578.
- [22] a) S.-W. Tsai, *J. Mol. Catal. B: Enzym.* **2016**, *127*, 98–116. b) P.-Y. Wang, C.-H. Wu, J.-F. Ciou, A.-C. Wu, S.-W. Tsai, *J. Mol. Catal. B: Enzym.* **2010**, *66*, 113–119. c) J. Pietruszka, R. C. Simon, F. Kruska, M. Braun, *Eur. J. Org. Chem.* **2009**, 6217–6224. d) A. Brodzka, D. Koszelewski, R. Ostaszewski, *J. Mol. Catal. B: Enzym.* **2012**, *82*, 96–101. e) S. Karlsson, C. Gardelli, M. Lindhagen, G. Nikitidis, T. Svensson, *Org. Proc. Res. Dev.* **2018**, *22*, 1174–1187.
- [23] P. Flores-Sánchez, J. Escalante, E. Castillo, *Tetrahedron: Asymmetry*, **2005**, *16*, 629–634.
- [24] H. Rangel, M. Carrillo-Morales, J. M. Galindo, A. Obregón-Zuñiga, E. Juaristi, J. Escalante, *Tetrahedron: Asymmetry*, **2015**, *26*, 325–332.
- [25] M. Pérez-Venegas, G. Reyes-Rangel, A. Neri, J. Escalante, E. Juaristi, *Beilstein J. Org. Chem.* **2017**, *13*, 1728–1734.
- [26] J. Escalante, F. D. Díaz-Coutiño, *Molecules* **2009**, *14*, 1595–1604.
- [27] M. Otsuka, T. Masuda, A. Haupt, M. Ohno, T. Shiraki, Y. Sugiura, K. Maeda, *J. Am. Chem. Soc.* **1990**, *112*, 838–845.
- [28] M. Brenner, D. Seebach, *Helv. Chim. Acta* **1999**, *82*, 2365–2379.
- [29] S. Yamamoto, S. Nakatani, M. Ikura, T. Sugiura, Y. Nishita, S. Itadani, K. Ogawa, H. Ohno, K. Takahashi, H. Nakai, M. Toda, *Bioorg. Med. Chem.* **2006**, *14*, 6383–6403.
- [30] L. Chang-Seok, K. Jong Sung, K. Ki Dong, K. Geun Tae, K. Kyoung-Hee, H. Sang Yong, K. Sungsub, K. Min-Jung, Y. Hyeon Joo, L. Dongchul, K. Hye Jin, H. Hee Oon, B. Seong Cheol, K. Oh Hwan, K. Ho Sung, H. Gwong-Cheung, K. Ji Young, Y. Zi-Ho, Y. Dong-Jun, *Y PCT Int. Appl.* **2006**, 197 CODEN: PIXXD2; WO2006104356.
- [31] K. Miyazawa, T. Koike, M. Akita, *Adv. Synth. Catal.* **2014**, *356*, 2749–2755.
- [32] J. M. García, M. A. Maestro, M. Oiarbide, J. M. Odriozola, J. Razkin, C. Palomo, *Org. Lett.* **2009**, *11*, 3826–3829.
- [33] Spartan'18. United States. Wavefunction Inc. 2019.
- [34] R. Thomsen, M. H. Christensen, *J. Med. Chem.* **2006**, *49*, 3315–3321.
- [35] W. Humphrey, A. Dalke, K. Schulten, *J. Molec. Graphics*, **1996**, *14*, pp. 33–38.
- [36] BIOVIA, Dassault Systèmes, [Discovery Studio Visualizer], [Discovery Studio 2019 Client], San Diego: Dassault Systèmes, [2019].

## FULL PAPER

## Entry for the Table of Contents



In contrast to *N*-protected  $\beta^3$ -amino esters, the *Candida antarctica* lipase B catalyzed kinetic resolution of amino esters holding alpha ( $\gamma^2$ ), beta ( $\gamma^3$ ), and gamma ( $\gamma^4$ ) stereocenters is strongly compromised by steric factors at the level of the catalytic cavity. Molecular docking studies helped establish that the steric exclusion region involves the Ile189 and Val190 residues and the amino bonding region where a hydrogen bond with the Asp134 residue is favored.